



# Facile synthesis of three-dimensional porous hydrogel and its evaluation

Zeeshan Danish<sup>1</sup> · Hira Ijaz<sup>2,3</sup> · Ghulam Razzaque<sup>4</sup> · Nauman ul Haq<sup>4</sup> · Muhammad Mahran Aslam<sup>5</sup>

Received: 25 March 2021 / Revised: 16 July 2021 / Accepted: 9 August 2021

© The Author(s), under exclusive licence to Springer-Verlag GmbH Germany, part of Springer Nature 2021

## Abstract

The aim of the current research work was to fabricate polymeric nexus for controlled delivery of metoprolol tartrate by using free radical polymerization. Polymer (aloe vera, sodium carboxymethyl cellulose, and meggletose) was crosslinked with monomer (acrylic acid) by using N,N methylene bisacrylamide. Swelling behavior was studied in pH 1.2 and 7.4. Sol gel fraction depicted gel fraction increased with the increase in feed ratio (polymer, monomer, and crosslinker). Optimized formulation was evaluated via Fourier transform infrared spectroscopy (FTIR) and scanning electron microscopy (SEM). FTIR confirmed compatibility of metoprolol with formulated system. Moreover, pH-dependent swelling was observed, experiencing significant swelling at higher pH. SEM depicted porous architecture which is responsible for swelling, drug loading, and release. Dissolution studies showed percentage drug release was significant in pH 7.4. Hence, the current research work demonstrates sustained delivery of metoprolol by employing varying concentration of polymer, monomer, and crosslinker. These fascinating properties made hydrogel a promising carrier for sustained drug delivery.

**Keywords** Aloe vera · Sodium carboxymethyl cellulose · Meggletose · Acrylic acid · Hydrogel

---

✉ Zeeshan Danish  
zeeshan.danish@pu.edu.pk

✉ Hira Ijaz  
pharmacisthira@gmail.com

<sup>1</sup> Faculty of Pharmacy, University of Punjab, Lahore, Pakistan

<sup>2</sup> College of Pharmacy, University of Sargodha, Sargodha, Pakistan

<sup>3</sup> Department of Pharmacy, University of Agriculture, Faisalabad, Pakistan

<sup>4</sup> Department of Pharmacy, University of Balochistan, Quetta, Pakistan

<sup>5</sup> Nuclear Institute of Agriculture (NIA) Tandojam, Sindh, Pakistan

## Introduction

Superporous network is 3-dimensional architecture of crosslinked hydrophilic polymer (copolymer or homopolymer) which imbibe significant quantity of water. Different pendent groups like amide, hydroxyl, amine, carboxylic acid, and sulfonic acid groups can be modified according to desired applications like drug targeting and release [1–3]. Superporous network formulated with various natural sources like aloe vera, cellulose is economical, biodegradable; moreover, intra-molecular and inter-molecular hydrogen bonds formation, cleavage aids in on–off switching [1]. Topological attributes, void fraction, pore size, pore size distribution, and interconnectivity of porous nexus also influence the swelling of nexus [2]. Superporous nexus has vast technological and scientific influence as they have inherent adsorption/absorption attributes which is related to interior as well as exterior interactions with atoms, ions, and molecules [3]. A range of systems such as rafts [4], scaffolds [5], polymeric carriers [6, 7], lipids [8] have been used as DDSs, but hydrogel depicts slow drug release; however, release can be improved via chemical crosslinking. At present, stimuli-responsive DDSs have been fascinating theme for controlled release. The release behaviors of drugs can be easily controlled by surrounding attributes such as pH, temperature, ionic strength, and electric field. Crosslinking of nexus is novel step to attain desire attributes like sophisticated architecture, good stability. Out of photo-crosslinking and enzymatic crosslinking, chemical crosslinking is widely used approach as it can be facilely realized through the enormous diversity of chemical structures from the hydrogel [9, 10].

Nowadays, many scientists urge the use of natural components like plant extract for therapeutic carrier. “Aloe” word is derived from arabic word “Alloeh” meaning “shinning bitter substance,” and “vera” is a latin word which means “true.” It contains 75 active components which include: vitamins (A, C, E, B12), enzymes (alkali phosphate, amylase, catalase, cellulase, lipase, peroxidase, bradykinase), sugars (glucose, fructose, glucomannan, and polymannose), hormones and fatty acids (gibberellin and auxin), steroids (campesterol, beta-sitosterol, cholesterol, and lupeol), minerals (calcium, chromium, magnesium, selenium, copper, potassium, zinc, and sodium), anthraquinones [11]. Aloe vera (AV) is water soluble, greater swelling which is attributed to hydrophilic nature. Due to its hydrophilic nature, it is widely explored pharmaceutical excipient in different dosage forms like hydrogels, niosomes, liposomes, nasal formulations [12]. Sodium carboxymethyl cellulose (NaCMC) is a water-soluble cellulose derivative which is biocompatible, biodegradable, and bioadhesive. Due to its polyelectrolyte nature, “smart” polysaccharide base polymer depicted pH sensitivity. NaCMC contains large number of hydroxyl and carboxylate moiety in macromolecular chains which forms multivalent ionic crosslinks. Literature supports the fact that NaCMC augments electrostatic charge within the nexus which further enhances the swelling capacity up to two folds [2]. Meggletose (lactose) contains galactose covalently bound to glucose. Lactose is attractive hydrophilic materials due to hydroxyl pendent moiety, which renders it compatible and aids in enormous functionality [13].

Acrylic acid (AA) is superabsorbent, pH-sensitive polyelectrolyte [14]. Literature survey supports the fact that AA base nexus exhibits electro-, thermo-, and pH-sensitive behavior. In addition, AA imparts greater thermal stability to nexus as compared to substrate [8]. N, N methylene bisacrylamide (MBA) is three-dimensional crosslinker which imparts greater mechanical strength to nexus as compared to other crosslinkers [15]. Acrylamide portion polymerizes with bisacrylamide of MBA resulting in crosslinked structure. Many polymers and copolymers are produced from these reactions which impart mechanical strength and toughness to the formed polymer. It maintains the gel structure and keeps it firm as it forms network when crosslinks with polyacrylamides rather than forming linear chains [16–18].

Metoprolol tartrate is an antagonist of  $\beta$ -adrenergic receptors (cardio selective) as it only antagonizes those amines that act at  $\beta_1$  receptors. Drug is completely absorbed after oral administration from the gastrointestinal tract. But due to extensive first-pass effect by the liver, most of the drug gets metabolized and only 40 to 50 percent of it remains available to impart therapeutic effect. Peak plasma levels are achieved within one to two hours after administration of the drug [19].

In this research study, attempt was made to formulate permanent superporous nexus by reacting different polymers with acrylic acid in the presence of crosslinker (MBA). Performance of various nexus was evaluated by using variable percentage of polymers, monomer, and crosslinker.

## Material and method

### Materials

Powdered aloe vera (AV), sodium carboxymethyl cellulose (NaCMC) meggletose (MT), acrylic acid (AA), potassium per sulfate (KPS), methylene bisacrylamide (MBA) procured from Sigma-Aldrich, Germany. These all materials were of high quality and pharmaceutical grade. All the other solvents and materials availed in formulations were of analytical grade.

### Synthesis of hydrogels using different polymers

Polymerization by free radical approach was used in the current study for preparing different formulations of hydrogels with varying quantities of reactants. Weighed amounts of polymers were added in predefined amount of distilled water with constant stirring to form clear solution. Then, KPS was added to this solution. Final volume of the solution was made 10 mL by the addition of distilled water. In this solution, varying amount of acrylic acid (AA) was added along with varying concentration of crosslinker (MBA). Above solutions were then mixed at room temperature of 25 °C, and final volume was made up to 20 ml with distilled water in Pyrex glass test tube having 16 mm diameter. Mouth of test tubes was then covered with glass cork. Test tubes with different formulations were set down in the water bath under nitrogen atmosphere to remove air. Temperature

of the water bath was gradually increased (45 °C for 1 h, 50 °C for 2 h, 55 °C for 3 h, 60 °C for 4 h, and 70 °C for 6 h) to prevent formation of air bubbles during gel formation. Test tubes were cooled and hydrogels formed were then removed from the glass test tubes and cut into circular discs each having 5 mm thickness. Water and ethanol in ratio of (9:1) were used for washing of cut discs for two weeks to remove any un-reacted monomer and initiator. Washing solution for discs was changed after every 12 h for two weeks. Drying of these washed discs was done at room temperature first and then placed in oven (Mettler, Universal oven UN55, Germany) at 45 °C until they attained sustained weight. These hydrogel discs were further saved in airtight labeled vials for physiochemical characterization [12, 15]. Different formulations of hydrogels (AV-*co*-AA, NaCMC-*co*-AA, and MT-*co*-AA) are given in Table 1. Presumptive diagram of AV-*co*-AA is shown in Fig. 1.

## Characterization

### Mechanical properties

A rod-shaped developed system of 4 mm diameter and 40 mm in length of fabricated AV-*co*-AA was taken in glass molds to execute its tensile strength. According to American Society of Testing Materials guidelines, tensile strength measuring equipment furnished with 10 kN load and TIRA software was used. A smooth surface sample was cut with the help of a specific cutter. The cut cylindrical rod was then fixed in between mobile and static jaws of the tensile tester. The mechanical tester was run at a speed of 50 mm/min in controlled environment. Young's modulus was determined taking slope from tensile stress–strain curve. Similarly, stress ( $\sigma$ ), i.e., force per unit area, and strain ( $\epsilon$ ), i.e., change in length, were determined by using the following expressions:

**Table 1** Different Formulations of Base Hydrogels

Formulation	Polymer (%)	AA (ml)	MBA (gm)	KPS (%)
AV1	1	15	0.15	0.04
AV2	1.5	15	–	0.04
AV3	2	15	–	0.04
AV4	2	20	0.1	0.04
NaCMC 1	1	15	0.15	0.04
NaCMC 2	1.5	15	–	0.04
NaCMC 3	2	15	–	0.04
NaCMC 4	2	20	0.1	0.04
MT1	1	15	0.15	0.04
MT2	1.5	15	–	0.04
MT3	2	15	–	0.04
MT4	2	20	0.1	0.04

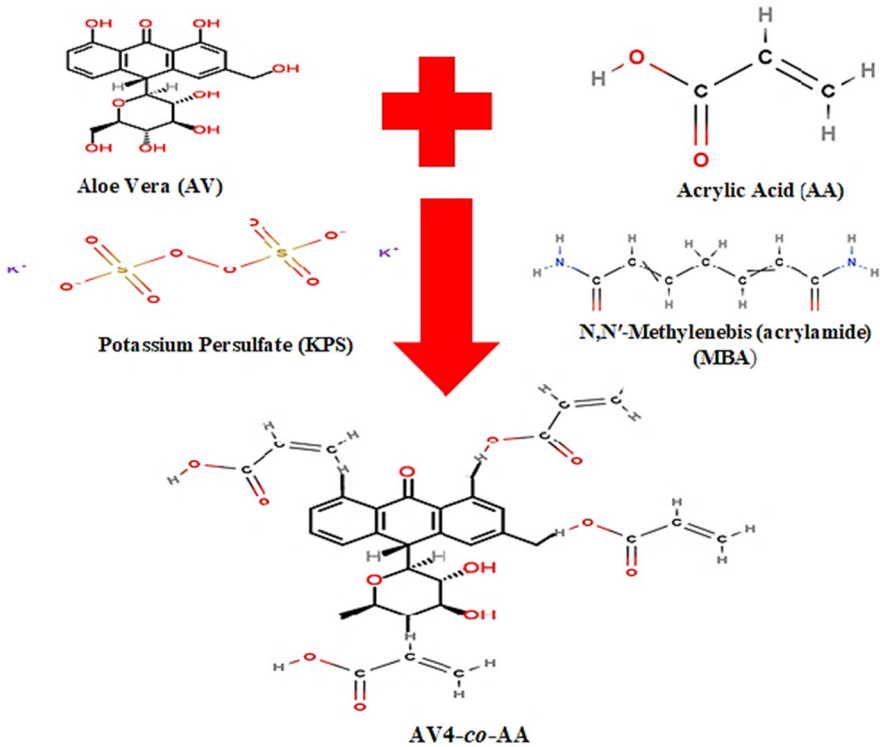


Fig. 1 Schematic diagram

$$\sigma = \frac{F}{\pi r^2}$$

where  $F$  = actual force applied,  $r$  = hydrogel radius and

$$\varepsilon = \frac{l_f - l_i}{l_i}$$

where  $l_i$  = initial length of hydrogel and  $l_f$  = final length of hydrogel [16].

### Fourier transform infrared spectroscopy (FTIR)

For obtaining infrared bands of formulated hydrogels, FTIR (FT-IR 8400 S, Shimadzu, Japan) was used. The crystal spot of FTIR was filled with formulated hydrogel's grounded powder, and then the sample was scanned in between  $4000 \text{ cm}^{-1}$  and  $600 \text{ cm}^{-1}$  wavelength [6–8].

## Scanning electron microscope (SEM)

For investigation of surface topology and morphology of drug-loaded hydrogels SEM was carried out by using scanning electron microscopy (Hitachi, S 3000 H, Japan). Scanning was done through 18 kV voltages in a distance of 10–25 mm [17].

## Swelling studies

### Dynamic swelling

To check the dynamic swelling, USP phosphate buffer having pH 7.4 and 1.2 was utilized. In these buffer solutions the dried hydrogel discs were placed that were pre-weighed, and the weights of hydrogel discs were calculated again after specific time period [13]. To check ratio of dynamic swelling following formula was used

$$q = W^h / W^d$$

where  $q$  = dynamic swelling,  $W^h$  = weight of swollen gel at time “t,”  $W^d$  = dry hydrogel preliminary weight.

### Equilibrium swelling

Hydrogel discs were allowed to swell for 15–20 days in USP phosphate buffer solutions of pH 1.2 and 7.4 till these hydrogel discs achieved persistent weight [14]. The following formula was utilized to calculate the ratio of equilibrium swelling ratio

$$V^{eq} = W^h / W^d$$

where  $V^{eq}$  = equilibrium swelling ratio,  $W^h$  = weight of swollen gel at time “t,”  $W^d$  = dry hydrogel preliminary weight.

### Sol–gel analysis

Polymer fraction that was uncrosslinked examined through sol–gel investigation. Soxhlet extraction of dried pre-weighed ( $W_o$ ) dried hydrogel discs were conducted for 4 h. The extracted hydrogel discs were dried initially at room temperature and then at 45 °C in oven until achieved constant weight ( $W_i$ ) [15]. By utilizing following formula calculation of sol–gel fraction was calculated

$$\text{Sol fraction (\%)} = W_o - W_i / W_o \times 100$$

$$\text{Gel fraction (\%)} = 100 - \text{sol fraction}$$

where  $W_0$  = dried hydrogels initial weight;  $W_1$  = after extraction weight of dried hydrogels.

### Porosity measurement

Hydrogels contain pores on their surface. Drug is released through these pores by diffusion. Porosity measurement was taken by the method of solvent replacement. Weighed dried disc of every formulated hydrogel was immersed in 100 mL absolute ethanol overnight. Discs were weighed again when excess of ethanol was seen on the surface. Percentage porosity was then computed by using formula [16].

$$\text{Porosity} = M2 - M1/PV$$

where  $M1$  = mass of hydrogel after immersion into ethanol;  $M2$  = mass of hydrogel before immersion into ethanol;  $P$  = density of ethanol solution l;  $V$  = volume of disc of hydrogel.

### On-off switching/pulsatile behavior

On-off switching or reversible swelling was representative of drug discharge in a measured way. To examine the pulsatile behavior of hydrogels, the discs were allowed to swell in pH 7.4, then deswelling at pH 1.2, and again swelling in pH 7.4 and deswell at pH 1.2 [17]

### Drug loading

“Swelling” is a method used for drug loading of formulated hydrogels in which hydrogel discs were dipped at room temperature into 1% (w/v) solution of metoprolol for 24 h until the discs were swollen. Drug-loaded disks were washed, blotted with filter paper, and dried in oven at 40 °C until they attained constant weight. Then these dried hydrogel discs was estimated through “weight method” by following formula [4, 20].

$$\text{Drug loading (\%)} = W_D - W_d / W_D \times 100$$

where  $W_D$  = after loading of drug hydrogels weight;  $W_d$  = dried hydrogels of initial weight. Another method used for drug loading was “extraction” in which frequent extraction with USP phosphate buffer solutions at pH 7.4 was done to evaluate quantity of drug loading through UV-visible spectrophotometer (UV-2700i Shimadzu, Japan) at 295–300 nm. Third method employed “swelling” for estimation of drug loading [9, 21].

### *In vitro* drug discharge studies

Dissolution of hydrogels was done by using USP phosphate buffer pH 7.4 and 0.1 N HCl (pH 1.2) at 37 °C in USP Type II dissolution apparatus (Pharmatest; type PT-DT 7, Germany). 900 mL dissolution media were used and paddle speed was set

at 100 rpm. At consistent interval, dissolution media of 5 mL quantity were withdrawn and replaced by fresh media to achieve persistent volume. Metoprolol release was checked through UV–visible spectrophotometer (UV-2700i Shimadzu, Japan) at 215 nm [18].

## Release kinetic analysis

### Model-dependent approach

To know about drug release phenomenon, different mathematical models were used like zero-order model, first-order model, Higuchi model, and Hixson–Crowell model Korsmeyer–Peppas model [5]

$$\text{Zero - order drug release} = F_t = \kappa_0 t$$

$F$  = fraction of drug release per unit time  $t$ ,  $\kappa_0$  = zero-order release constant.

$$\text{First - order drug release} = \ln(1 - F) = -\kappa_1 t$$

$F$  = fraction of drug release in time,  $\kappa_1$  = first-order release constant.

$$\text{Higuchi model} = F = \kappa_2 t^{1/2}$$

$F$  = fraction of drug release in time  $t$  and  $\kappa_2$  = Higuchi constant.

$$\text{Hixson crowell model} = W_0^{1/3} - W_t^{1/3} = \kappa t$$

$W_0^{1/3}$  is the initial amount of drug in the hydrogel,  $W_t^{1/3}$  is remaining amount of drug in the hydrogel at  $t$ , and  $\kappa$  is a constant

$$\text{Korsmeyer - Peppas model} = M_t/M_\infty = \kappa_3 t^n$$

$M_t$  = penetrant time ( $t$ ),  $M_\infty$  = amount of water at equilibrium,  $\kappa_3$  = kinetic constant, and

$n$  = exponent depicting swelling mechanism.

### Model independent approach

Model independent approach requires similarity ( $f_2$ ) and difference factor ( $f_1$ )

$$f_2 = 50 \log \{ [1 + (1/n) S t = 1n(Rt - Tt)2] - 0.5 \times 100 \}$$

$$f_1 = \{ [St = 1n|Rt - Tt|] / [St = 1nRt] \} \times 100$$

### Statistical approach

The experiment results were assessed through ANOVA (analysis of variance) single factor by SPSS-16.



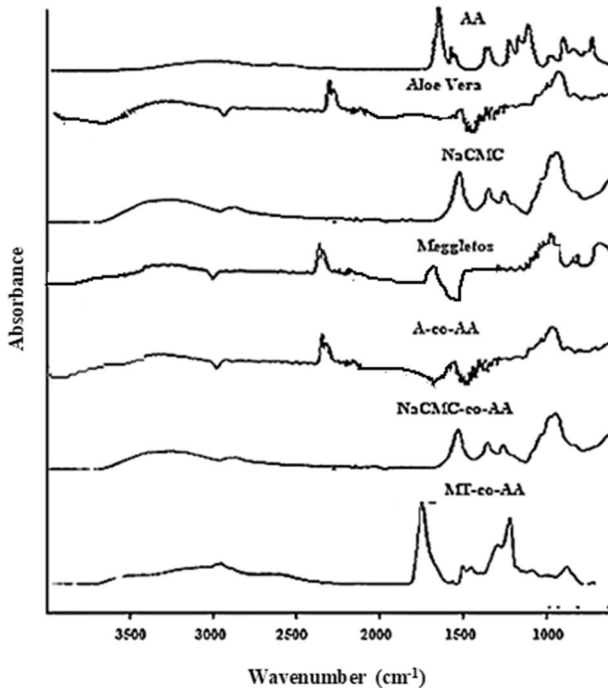


Fig. 2 FTIR of AA, AV, NaCMC, MT, AV4, NaCMC4, and MT4

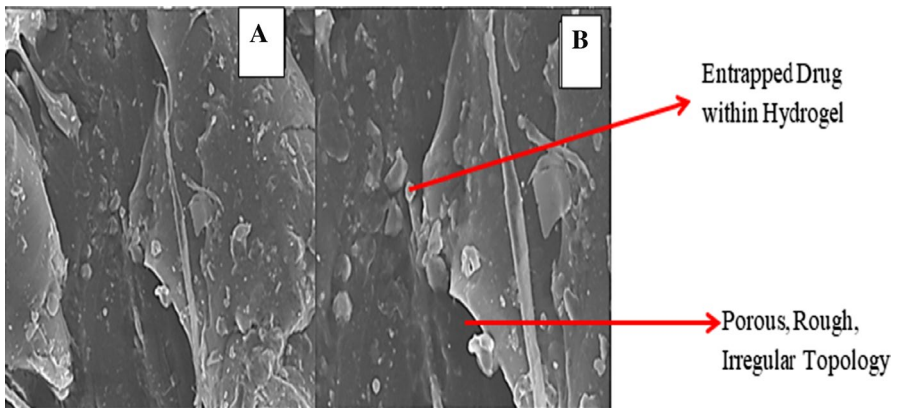


Fig. 3 Scanned micrographic image of drug-loaded aloe vera hydrogel at magnification 100X (a), 500X (b)

## Results and discussion

Results of formulated hydrogel are shown in Figs. 2, 3, 4, 5, 6, 7, 8, 9, 10, 11, 12, 13, 14, 15, and 16 and Tables 2, 3

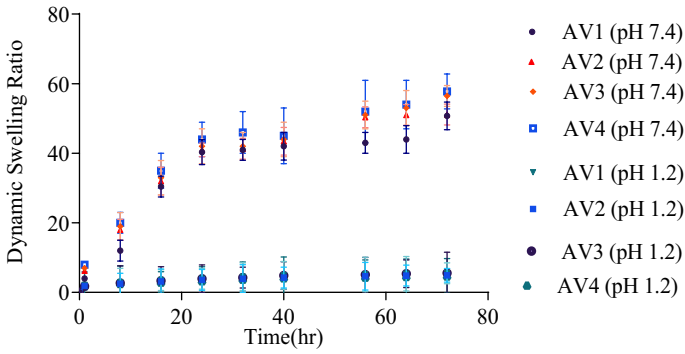


Fig. 4 Dynamic swelling ratio of AV1-AV4 in pH 1.2 and pH 7.4

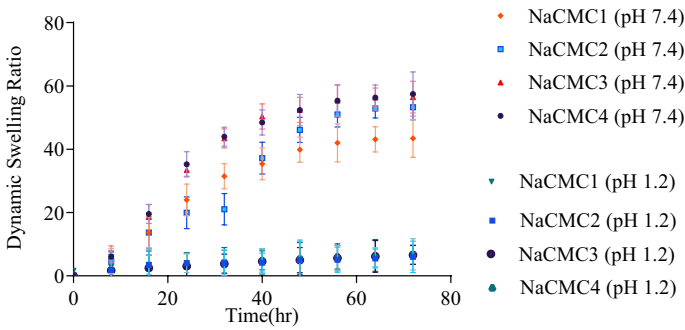


Fig. 5 Dynamic swelling ratio of NaCMC1-NaCMC4 in pH 1.2 and pH 7.4

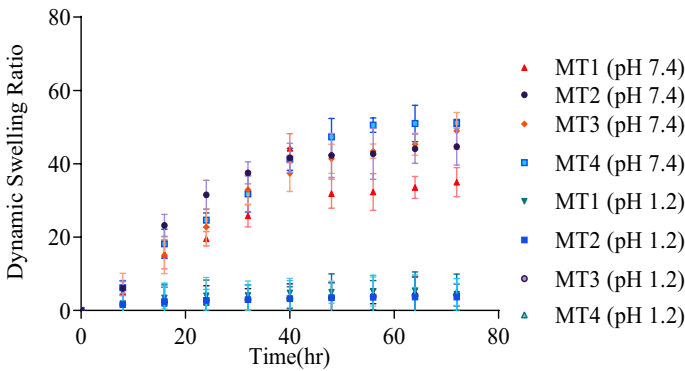


Fig. 6 Dynamic swelling ratio of MT1-MT4 in pH 1.2 and pH 7.4

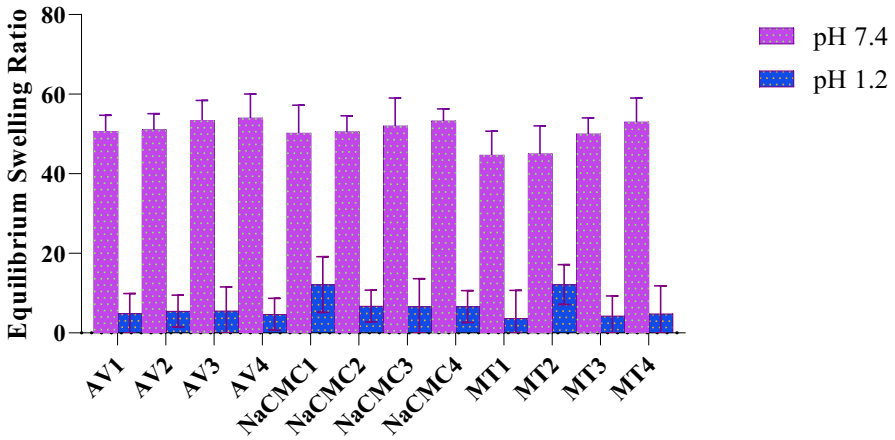


Fig. 7 Equilibrium swelling ratio in pH 1.2 and pH 7.4

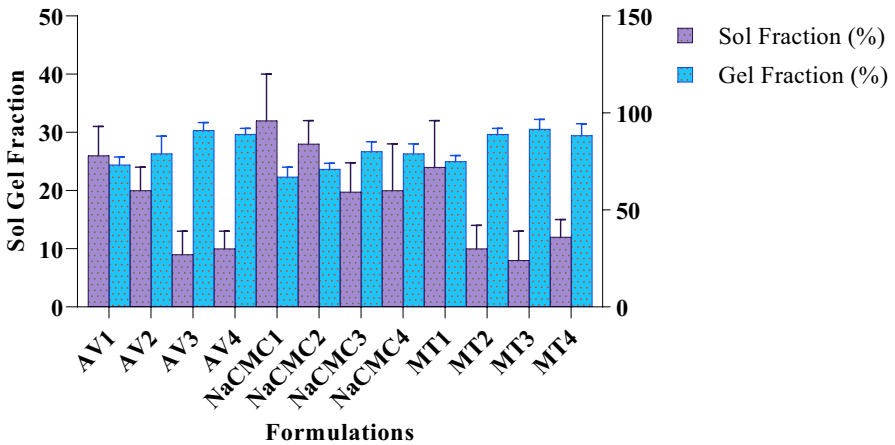


Fig. 8 Sol-gel fraction of all formulations

### Mechanical properties

The mechanical properties of developed network were evaluated by using tensile test. AV4 hydrogel demonstrated extraordinary mechanical properties with tensile strength of  $38.224 \text{ N/mm}^2$ . Formulated hydrogel had a significant stiffness, presenting a Young's modulus as much as  $244.94 \text{ N/mm}^2$ , and percentage total elongation at maximum force was 18.586%. The load at the time of break was observed to be 4.911 N.

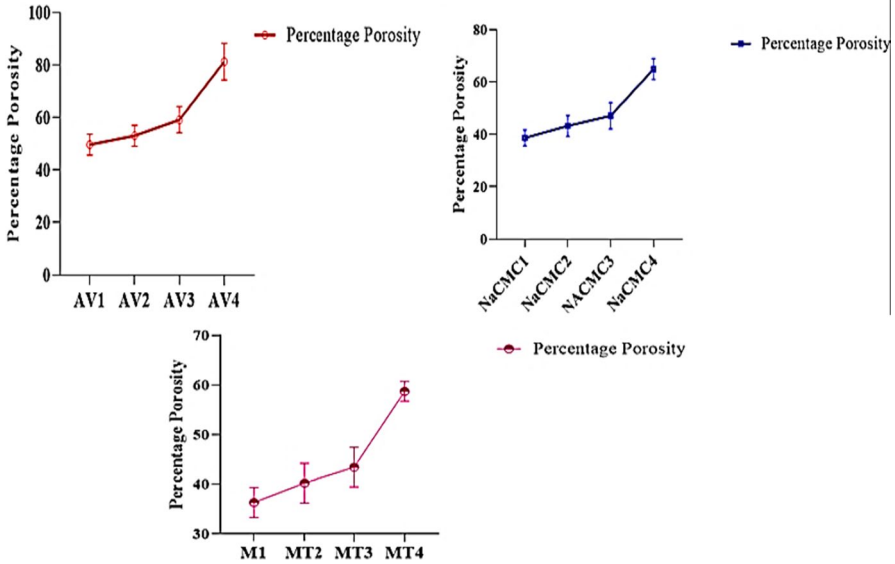
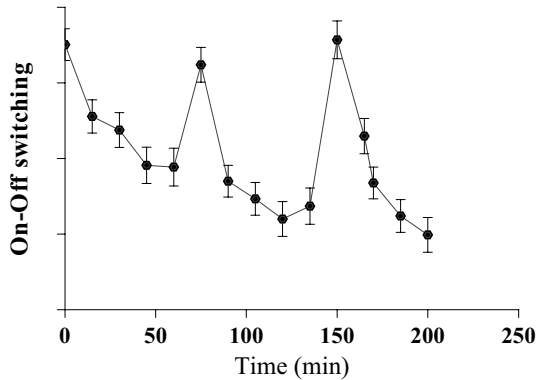


Fig. 9 Porosity measurement of all formulations

Fig. 10 On-off switching of AV4 in pH 1.2 and pH 7.4



### FTIR Spectroscopy

Spectra of aloe vera showed peak corresponding to asymmetrical  $\text{COO}^-$  stretching at  $1722\text{ cm}^{-1}$ , glycosidic bond peak at  $1600\text{ cm}^{-1}$ , and  $\text{CH-}$  ring vibration at  $850.53\text{ cm}^{-1}$ . Similar peaks are observed by Chauhan & Kumar (2018) while microbial coating of cellulosic while using aloe vera [22]. Spectra of NaCMC showed  $\text{OH-}$  stretching vibration at  $3443.8\text{ cm}^{-1}$ , a band showing ether bonds at  $1000\text{--}1166.6\text{ cm}^{-1}$ , absorption peak of carboxylate at group at  $1635\text{ cm}^{-1}$ , and a peak at  $2926.8\text{ cm}^{-1}$  showed methylene moiety. These peaks are also evident from research work of Adinugraha and Marseno (2005) [23]. Spectra of meggletose clearly presented sharp  $\text{OH-}$  stretch peaks at  $3521.5\text{ cm}^{-1}$  which corresponded to

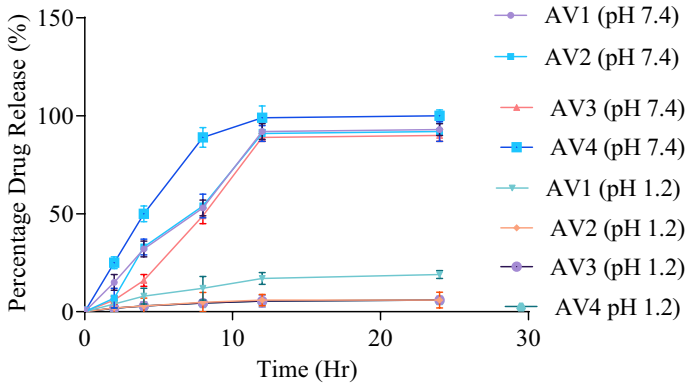


Fig. 11 Percentage drug release from AV1 to AV4 in pH 1.2 and pH 7.4

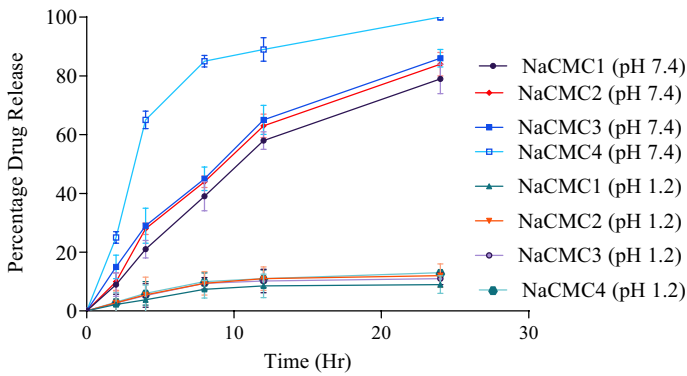


Fig. 12 Percentage drug release from NaCMC1 to NaCMC4 in pH 1.2 and pH 7.4

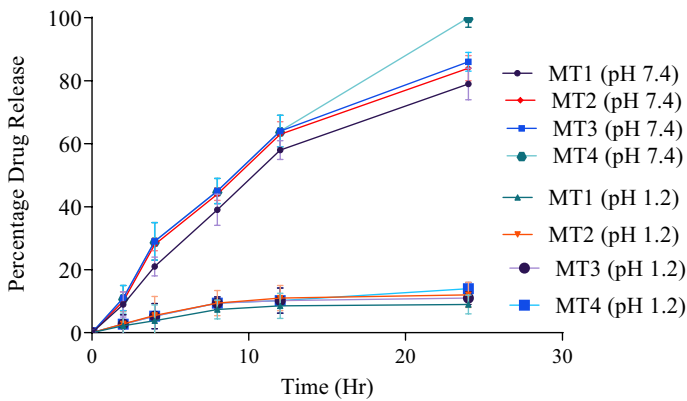


Fig. 13 Percentage drug release from MT1 to MT4 in pH 1.2 and pH 7.4

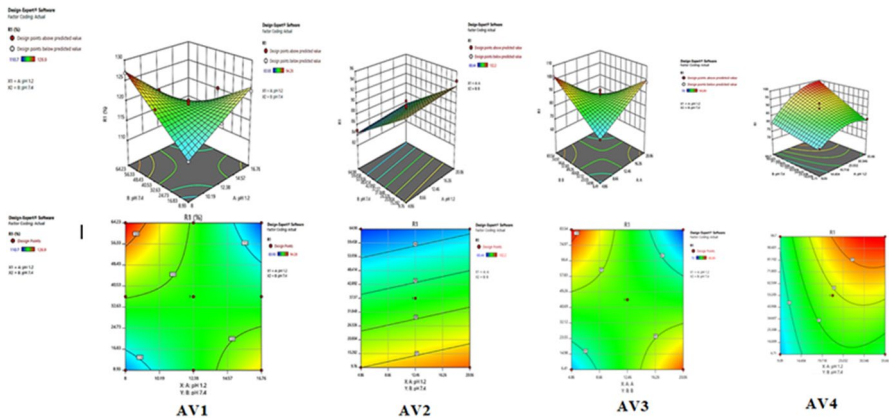


Fig. 14 RSM graph and contour plots of formulation AV1-AV4

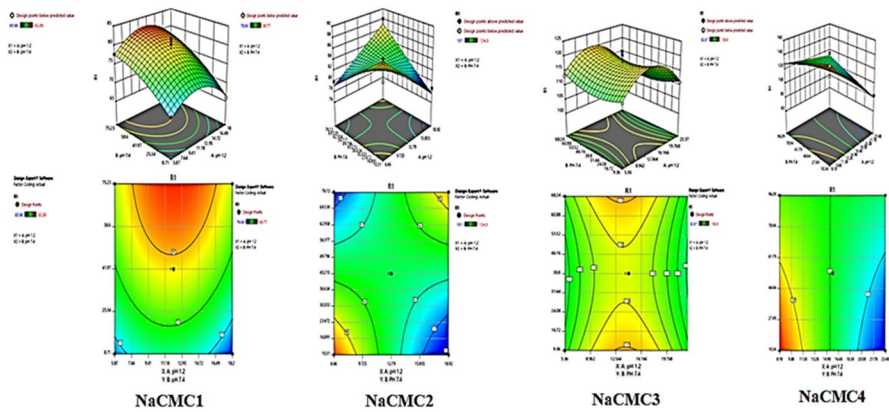


Fig. 15 RSM graph and contour plots of formulation NaCMC1-NaCMC4

OH– group. IR spectrogram also showed distortion of water molecule at  $1600\text{ cm}^{-1}$ , which confirmed the presence of water molecule in the crystal of lactose (meggletose). Acrylic acid IR spectrogram was studied, and a broad peak representing  $\text{OH}^-$  stretching was observed at almost  $3445\text{ cm}^{-1}$ , peak of  $\text{CH}^-$  group at  $2933\text{ cm}^{-1}$ , and bending of  $\text{C}=\text{O}$  of  $-\text{COOH}$  at  $1573\text{ cm}^{-1}$  as observed earlier by Ijaz et al., 2020 [15]. These individual IR spectra of components were compared with the drug-loaded formulations (Fig. 2). Spectra of loaded formulations showed no major shift in the absorption peaks ascertaining that no chemical interaction has taken place between the substrate.

### Scanning electron microscopy

To study the morphology of surface of formed hydrogels, SEM was performed on hydrogels loaded with metoprolol tartrate (AV4 (AV-co-AA) at different

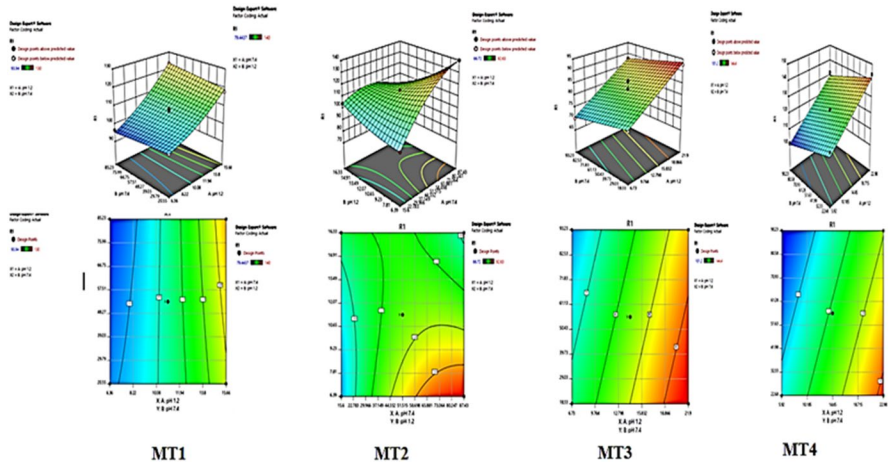


Fig. 16 RSM graph and contour plots of formulation MT1-MT4

Table 2 Drug loaded in formulated hydrogel

Drug loading	By swelling (mg/gm)	By weight (mg/gm)	By extraction (mg/gm)
AV1	62 ± 0.34	60 ± 0.34	50 ± 0.23
AV2	69 ± 0.34	64 ± 0.23	60 ± 0.46
AV3	71 ± 0.24	69 ± 0.12	68 ± 0.65
AV4	72 ± 0.39	70 ± 0.13	72 ± 0.36
NaCMC1	62 ± 0.39	64 ± 0.33	60 ± 0.34
NaCMC2	63 ± 0.25	68 ± 0.24	64 ± 0.27
NaCMC3	69 ± 0.12	72 ± 0.14	69 ± 0.12
NaCMC4	70 ± 0.13	78 ± 0.13	70 ± 0.13
MT1	61 ± 0.34	59 ± 0.34	61 ± 0.31
MT2	62 ± 0.28	63 ± 0.23	69 ± 0.32
MT3	69 ± 0.18	69 ± 0.12	72 ± 0.24
MT4	70 ± 0.13	70 ± 0.13	72 ± 0.34

resolutions. Figure 10 shows the presence of numerous pores on the gel surface. This fibrous and sponge-like structure is due to interpenetrating networks present in the gel matrix. Figure 3 indicates the incorporation of loaded drug in these pores which is dispersed throughout the hydrogel. Drug release depends on the swelling ratio, polymer interaction with other substrate (AA and MBA). Pore inter-connectivity and architecture plays vital role in swelling and de-swelling of polymeric nexus [10]. However, drug-loaded solution enters the porous nexus via convection, thereby improving entrapment efficacy of drug [24, 25].

**Table 3** Kinetic model of drug release in pH 1.2 and 7.4

Model	pH	AV1	AV2	AV3	AV4	NaCMC1	NaCMC2	NaCMC3	NaCMC4	MT1	MT2	MT3	MT4
Zero order	7.4	$R^2$	0.99	0.89	0.99	0.99	0.99	0.99	0.98	0.98	0.99	0.97	0.99
	1.2	$R^2$	0.82	0.71	0.74	0.91	0.91	0.89	0.89	0.89	0.74	0.91	0.91
First order	7.4	$R^2$	0.62	0.50	0.64	0.60	0.55	0.58	0.62	0.50	0.64	0.60	0.55
	1.2	$R^2$	0.59	0.64	0.66	0.56	0.56	0.50	0.50	0.50	0.66	0.56	0.56
Higuchi model	7.4	$R^2$	0.93	0.97	0.93	0.95	0.96	0.89	0.99	0.93	0.93	0.95	0.96
	1.2	$R^2$	0.95	0.91	0.94	0.92	0.93	0.94	0.94	0.99	0.94	0.92	0.93
Hixson–Crowell model	7.4	$R^2$	0.95	0.98	0.95	0.98	0.98	0.71	0.95	0.98	0.95	0.98	0.98
	1.2	$R^2$	0.83	0.71	0.75	0.98	0.98	0.98	0.98	0.98	0.75	0.98	0.98
Korsmeyer–Peppas model	7.4	$R^2$	0.91	0.80	0.92	0.89	0.85	0.86	0.91	0.93	0.92	0.89	0.85
	1.2	$R^2$	0.89	0.93	0.95	0.86	0.86	0.80	0.80	0.80	0.95	0.86	0.86



## Swelling studies

### Effect of pH on the swelling

pH of GIT track varies from acidic (stomach) to basic (intestine). pH of the medium and pKa are the two crucial factors that play significant role in the swelling of the hydrogels. The buffer will accept the protons and ionize the hydrogel only if the pKa value of buffer components is above the pKa value of gel carboxylic group, resulting in efficient swelling. Ionization of the carboxylic group varies with the variation in the pH of the surrounding fluid and that influences the ability of hydrogels to swell. Increase in pH of the medium above the pKa values of the acidic constituent of hydrogel causes increase in ionization of carboxylic group resulting in swelling of the gels. Hydrogels swell as the pH increases; this is due to the ionic repulsion of protonated carboxylic groups, while they sag at low pH because of the presence of carboxylic groups which are unprotonated. Gupta et al. 2012 also investigated the same phenomenon. Maximum swelling was observed in gels immersed in phosphate buffer, while little or no swelling was observed in gels immersed in acidic medium [26]. Reduced swelling is seen at lower pH (<3) as most of the carboxylic moieties do not get protonated at this pH and so main anion–anion repulsive forces are eliminated. At higher pH values of (>4) some of the carboxylic groups start to get protonated and the electrostatic repulsion between COO<sup>-</sup> results in increased swelling of the hydrogels. It is observed that more of drug is released in basic medium that is in phosphate buffer of pH 7.4 as compared to 0.1 N HCl. This is because hydrogels built high osmotic pressure inside them at higher pH values when compared to lower pH values. This high built in pressure causes maximum release of drug from the matrix. Moreover, at higher pH all carboxylic groups are transforming in to salt form which results in augmented swelling in pH 7.4. Influence of pH on swelling is shown in Figs. 4, 5 and 6.

### Effect of monomer (acrylic acid) on swelling

Acrylic acid, a polyelectrolyte, naturally available superabsorbent is responsive to pH. Carboxylic group present in acrylic acid reacts with the aqueous phase and gets ionized readily at higher pH values. Hydrogels having different concentrations of acrylic acid, i.e., 15 and 20 mL (formulation AV3, AV4, NaCMC3, NaCMC4, MT3, and MT4), were prepared to investigate the effect of acrylic acid on swelling behavior of these hydrogels. It was noted at pH 7.4, swelling of gels increased in the formulations AV4, NaCMC4, and MT4 as there is increase in concentration of acrylic acid because more carboxylic groups are present to get ionized to form carboxylate ions, thus increasing the repulsion between the networks. Aloe vera-based formulations (AV3 and AV4) containing 15 and 20 mL acrylic depicted ESR of  $53.03.49 \pm 0.24$  and  $56.78 \pm 0.23$ . However, NaCMC-based formulation (NaCMC3 and NaCMC4) containing 15 and 20 mL AA depicted ESR of  $52.03 \pm 0.24$  and  $53.29 \pm 0.23$ . Lactose-based formulation MT3 and MT4 containing 15 and 20 mL AA showed ESR of  $50.98 \pm 0.24$  and  $52.22 \pm 0.24$ , respectively. The pKa value of acrylic acid is said to be 4.28; consequently, diminished swelling is observed at pH

1.2 because acrylic acid chains are in crumpled state and electrostatic forces are very strong. Majeed et al. 2020 prepared pH-sensitive gelatin/polyvinylpyrrolidone-co-poly(acrylic acid)-based nexus and reported the similar fact [24].

### Effect of polymer concentration on swelling

Formulations having varying polymer concentrations were synthesized by using AV, NaCMC, and MT. Figures 4, 5, 6 and 7 show that as the concentration of the polymer increases, swelling of the hydrogel increase both in pH 1.2 and pH 7.4 provided that concentration of acrylic acid and crosslinker is kept constant. The same observations were made in both equilibrium and dynamic equilibrium state studies. Formulation AV1-AV3 containing 1, 1.5, and 2% aloe vera showed significant increment in ESR ( $50.71 \pm 0.23$ ,  $51.31 \pm 0.45$ , and  $53.03 \pm 0.45$ ) in pH 7.4. Formulation NaCMC1 – NaCMC3 containing 1, 1.5, and 2% NaCMC showed ESR of  $50.54 \pm 0.65$ ,  $50.78 \pm 0.34$ , and  $53.03 \pm 0.24$ . Formulation MT1-MT3 showed significant increment in swelling ratio.

### Effect of crosslinker on swelling

To determine the effect the crosslinker on swelling, one formulation of each polymer was made having increased concentration of crosslinking agent. It was observed that swelling of hydrogels decreased by increasing the content of crosslinking agent in both dynamic and static equilibrium studies in acidic and basic medium. Formulation AV4, NaCMC4, and MT4 containing least concentration (0.1%) of MBA showed significant increment in swelling. Drug release was also slowed down by increase in crosslinker concentration. This effect can be justified by the reason that more entanglement between the chains of polymeric matrix results by increasing the MBA concentration. Hydrogels which have high concentration of crosslinkers are closely packed, and their carboxylic groups are masked inside. So, less ionization takes place and thus they are less acidic. Similar results were put forward by Gami et al., 2020 while preparing 5-fluorouracil and curcumin-loaded xylan- $\beta$ -cyclodextrin nexus [25]. Reason of decreased in swelling ratio was considered as the physical entanglement that happened between mesh of polymeric networks. The polymeric networks having carboxylic group with a specific crosslinker were the reason of reduction in polymeric chain relaxation and result in decreased swelling ratio. Decreased swelling attributed toward higher concentration of MBA, ionized carboxylic group, hydrogen bonding between new fractions and functional groups having electrostatic forces between them [24].

### Sol–Gel analysis

Sol–gel analysis was done for all the formulations to determine the uncrosslinked fraction in each formed hydrogel. Sol–gel fraction shows direct relation with concentration of the polymers, monomer, and crosslinker. Figure 8 shows that gel fraction of hydrogels increased by increasing the concentration of polymer, monomer, and crosslinker as in formulations AV1, AV2, AV3, NaCMC1, NaCMC2, NaCMC3,

MT1, MT2, and MT3, while gel fraction decreased in A4, NaCMC4, and MT4 as concentration of crosslinking agent was reduced in these formulations. Formulation AV4, NaCMC4, and MT4 showed  $89.21 \pm 0.87$ ,  $79.93 \pm 0.45$ ,  $88.45\%$  gel fraction, and  $10.79 \pm 0.65$ ,  $20.07 \pm 0.65$ , and  $11.55 \pm 0.23\%$  sol fraction. The same fact was presented by Gami et al., 2020, while formulating xylan- $\beta$ -cyclodextrin nexus [25]

### Porosity measurement

Figure 9 indicates concentration of polymer and acrylic acid has direct effect on porosity of hydrogels, i.e., by the increase in acrylic acid or polymer, porosity also increases. This is because by increasing polymer and monomer, viscosity of the solution increases, and interconnected channels are formed which in turn prevents the bubbles from escaping, thus increasing the porosity, whereas, increasing the concentration of MBA, the crosslinking agent, porosity decreases because of less pore formation due to more entanglement between polymer and monomer. Formulation A4 has  $81.36 \pm 0.034\%$  porosity as compared to formulation NaCMC4 and MT4 which has percentage porosity of  $64.93 \pm 0.76$  and  $58.71 \pm 0.54$ , respectively. However NaCMC4 and MT4 base hydrogel depicted maximum porosity in their respective batches (NaCMC1, NaCMC2, NaCMC, MT1, MT2, and MT3). These results are same as demonstrated by Akhlaq et al., 2020 while formulating methotrexate-loaded pH-sensitive nexus [27].

### On–Off switching

Studies were performed to check reversible swelling effect. Swelling de-swelling was carried out at basic pH (7.4) and acidic pH (1.2). Higher swelling capability was observed at alkaline pH of 7.4 as shown in Fig. 10. Crosslink density in AV4 was negligible at low concentration of MBA, and results in formulated nexus have significant capacity to imbibe water. Carboxylic group changed into carboxylate ions at pH less than 7 [18]. Due to remarkable charge density of carboxylate group in polymer causes increase in osmotic pressure in hydrogels networks that cause  $-\text{COO}^-$ – $-\text{COO}^-$  repulsion through electrostatic forces. H-bond formation and its breakage resulted into on–off switching. When repulsion of ionized groups occurs, then it produces expansion in the crosslinked network of hydrogels. When water enters into hydrogels, then it generates osmotic pressure within it and thus expansion results. At lower pH, minor swelling occurs because carboxylic groups were protonated which cause hurdles to uptake water [24]. Abad et al., 2003, postulated the similar fact while formulating synthesized PVP-kappa carrageenan-based hydrogel blends [28].

### Drug loading

Acrylic acid (AA) and polymers are hydrophilic in nature, and loading of drug increased by increasing hydrophilic components, thereby increasing the ability of nexus to absorb in drug solution, whereas MBA concentration has an inverse relation because enhanced density causes decrease in penetration of drug solution [22]. Drug loading is shown in Table 2. AV1, AV2, AV3 with

higher concentration of crosslinker (0.15 gm) showed drug loading of  $62 \pm 0.34$ ,  $69 \pm 0.34$ ,  $71 \pm 0.24$  mg/0.45 gm of hydrogel, and A4 containing 0.1 gm MBA showed drug loading of  $72 \pm 0.39$  mg/0.45 gm of hydrogel. NaCMC1-NaCMC3 formulated with 0.15 gm MBA showed drug loading between  $62 \pm 0.39$  and  $69 \pm 0.12$  mg/0.45 gm of hydrogel. NaCMC4 containing 0.1 gm MBA showed drug loading of  $70 \pm 0.13$  mg/0.45 gm of hydrogel. Formulation MT1 to MT3 containing 0.15 gm MBA showed drug loading between  $61 \pm 0.34$  and  $69 \pm 0.18$  mg/0.45 gm of hydrogel. MT4 containing 0.1 gm MBA showed maximum drug loading of  $70 \pm 0.13$  mg/0.45 gm of hydrogel.

### Kinetics of release of drug

Drug release was observed in both acid and basic environments using 0.1 N HCl of pH 1.2 and 0.05 M USP phosphate buffer of pH 7.4 as shown in Figs. 11, 12, 13, 14, 15 and 16. Drug release increase with increase in pH as reported by Bashir et al., 2017 formulated pH responsive N-Succinyl chitosan-*g*-poly (acrylamide-*co*-acrylic acid) hydrogels and observed 16 and 86% theophylline release in pH 1.2 and 7.4 respectively. Swelling increase in pH 7.4, drug release increase proportionally [29, 30]. From Fig. 11, 12 and 13 it was observed that drug release showed direct relationship with ratio of polymer, monomer and indirect relationship with crosslinker concentration. Ijaz et al., 2018 formulated XG-*co*-PAA based nexus for controlled delivery of perindopril erbumine and observed similar fact [31]. Release pattern of drug was studied by applying zero, first order, Higuchi and Korsmeyer-Peppas models on the obtained release data. A criterion for selecting most appropriate model was regression coefficient. Value of (R) which is nearer to 1 is considered as the ideal model. Table 3 show the values of regression coefficient for formulations having varying amount of acrylic acid, MBA and polymers. It was observed that the values of R for most formulations of AV, NaCMC and MT were higher in case of zero order kinetic model than first order release rates. Increase in polymer and AA ratio, shift the release kinetics from first to zero order as indicated in formulations AV3, AV4, NaCMC3, NaCMC4, MT3 and MT4. Values of R in Higuchi model; having different concentration of acrylic acid and crosslinking agent, exhibited that drug which is released from the polymeric matrix is diffusion controlled. A4 and NaCMC4 formulations were same in the case as they both have similarity factor ( $f_2$ ) of 96.38 which is exactly as recommended by USA FDA. Difference factor ( $f_1$ ) also shows very minor difference in the readings of these two hydrogels. ANOVA single factor was used to have the statistical analysis with P value = 0.0479 lesser than 0.05 it reflects that the dissolution studies were significant [11]. Figure 14, 15 and 16 showed RSM graph and contour plots of all formulations.

### Conclusion

pH-sensitive hydrogel was formulated using free radical polymerization. A different polymer with different feed ratio was grafted with AA by using MBA. Maximum swelling and release was observed for formulation AV4 which showed drug release

up to 24 h. SEM results showed sponge-like structure on to which drug, metoprolol tartrate, was seen dispersed throughout the structure. Hydrogels formed in this present work showed the intended results. It was therefore concluded from this study that hydrogels based on aloe vera are pH sensitive and can serve as controlled delivery system for administering of sensitive biomolecules like proteins, peptide, etc.

## References

1. Bao Y, Ma J, Li N (2011) Synthesis and swelling behaviors of sodium carboxymethyl cellulose-g-poly (AA-co-AM-co-AMPS)/MMT superabsorbent hydrogel. *Carbohydr Polym* 84:76–82
2. Akalin O, Pulat M (2018) Preparation and characterization of nanoporous sodium carboxymethyl cellulose hydrogel beads. *J Nanomater*. <https://doi.org/10.1155/2018/9676949>
3. Liu P, Zhai M, Li J, Peng J, Wu J (2002) Radiation preparation and swelling behavior of sodium carboxymethyl cellulose hydrogels. *Radiat Phys Chem* 63:525–530
4. Biswas S, Biswas A, Galluzzi M, Shekh M, Wang Q, Ray B, Stadler FJ (2020) Synthesis and characterization of novel amphiphilic biocompatible block-copolymers of poly (N-isopropylacrylamide)-b-poly (L-phenylalanine methyl ester) by RAFT polymerization. *Polym* 203:122–760
5. Shekh M, Amirian J, Stadler F, Du B, Zhu Y (2020) Oxidized chitosan modified electrospun scaffolds for controllable release of acyclovir. *Int J Biol Macromol* 151:787–796
6. Dhanavel S, Praveena P, Narayanan V, Stephen A (2020) Chitosan/reduced graphene oxide/Pd nanocomposites for co-delivery of 5-fluorouracil and curcumin towards HT-29 colon cancer cells. *Polym Bull* 77:5681–5696
7. Dhanave S, Revathy A, Sivaranjani T, Sivakumar K, Palani P, Narayanan V, Stephen A (2020) 5-Fluorouracil and curcumin co-encapsulated chitosan/reduced graphene oxide nanocomposites against human colon cancer cell lines. *Polym Bull* 77:213–233
8. Ganna S, Raja S, Reddy G, Deva P, Raju B, Kummara M, Koduru M, John S (2021) Formulation, optimization, and in vitro characterization of omega-3-rich binary lipid carriers for curcumin delivery: in vitro evaluation of sustained release and its potential antioxidant behavior. *Polym Bull* 1:1–24
9. Amirian J, Zeng Y, Shekh M, Sharma G, Stadler F, Song J, Zhu Y (2021) In-situ crosslinked hydrogel based on amidated pectin/oxidized chitosan as potential wound dressing for skin repairing. *Carbohydr Polym* 251:117–125
10. Shahzadi K, Xiong W, Shekh M, Stadler F, Yan Z (2020) Fabrication of highly robust and conductive ion gels based on the combined strategies of double-network, composite, and high-Functionality cross-linkers. *ACS Appl Mater Inter* 12:49050–49060
11. Nayak A, Hasnain M, Dhara A, Pal, D (2021). (eds) *Bioactive Natural Products for Pharmaceutical Applications*. Advanced Structured Materials. Springer, Cham
12. Shiva K, Mandal S, Kumar S (2021) Formulation and evaluation of topical antifungal gel of fluconazole using aloe vera gel. *Int J Sci Res Develop* 1:187–193
13. Fonseca L, Dirlam P, Hillmyer A (2020) Atom-economical, one-pot, self-initiated photopolymerization of lactose methacrylate for biobased hydrogels. *ACS Sustain Chem Eng* 8:4606–4613
14. Jin X, Hsieh Y (2005) pH-responsive swelling behavior of poly (vinyl alcohol)/poly (acrylic acid) bi-component fibrous hydrogel membranes. *Polym* 46:5149–5160
15. Ijaz H, Tulain U, Minhas M, Mahmood A, Sarfraz R, Erum A, Danish Z (2020) Design and in vitro evaluation of pH-sensitive crosslinked chitosan-grafted acrylic acid copolymer (CS-co-AA) for targeted drug delivery. *Int J Polym Mater* 5:1–13
16. Ijaz H, Tulain U (2019) Development of interpenetrating polymeric network for controlled drug delivery and its evaluation. *Int J Polym Mater* 5:1099–1107
17. Zhong M, Liu T, Xie M (2015) Self-healable, super tough graphene oxide–poly (acrylic acid) nanocomposite hydrogels facilitated by dual cross-linking effects through dynamic ionic interactions. *J Mat Chem B* 3:4001–4008
18. Tayyab A, Mahmood A, Ijaz H, Sarfraz R, Zafar N, Danish Z (2020) Formulation and optimization of captopril-loaded microspheres based compressed tablets: in vitro evaluation. *Int J Polym Mater* 6:1–13

19. Ijaz H, Qureshi J, Danish Z, Zaman M, Abdel-Daim M, Hanif M, Mohammad I (2015) Formulation and in-vitro evaluation of floating bilayer tablet of lisinopril maleate and metoprolol tartrate. *Pak J Pharm Sci* 28:2019–2025
20. Ijaz H, Qureshi J, Danish Z, Zaman M, Abdel-Daim M, Bashir I (2017) Design and evaluation of bilayer matrix tablet of metoprolol tartrate and lisinopril maleate. *Adv Polym Tech* 36:152–159
21. Mahmood A, Ahmad M, Sarfraz R, Minhas M (2016)  $\beta$ -CD based hydrogel microparticulate system to improve the solubility of acyclovir: optimization through in-vitro, in-vivo and toxicological evaluation. *J Drug Deliv Sci Technol* 36:75–88
22. Chauhan P, Kumar A (2020) Development of a microbial coating for cellulosic surface using aloe vera and silane. *Carbohydr Polym Tech App* 1:1000–1015
23. Adinugraha M, Marseno D (2005) Synthesis and characterization of sodium carboxymethylcellulose from cavendish banana pseudo stem (*Musa cavendishii* LAMBERT). *Carbohydr Polym* 62:164–169
24. Majeed A, Pervaiz F, Shoukat H, Shabbir K, Noreen S, Anwar M (2020) Fabrication and evaluation of pH sensitive chemically cross-linked interpenetrating network [Gelatin/Polyvinylpyrrolidone-copoly (acrylic acid)] for targeted release of 5-fluorouracil. *Polym Bull* 12:1–20
25. Gami P, Kundu D, Seera S, Banerjee T (2020) Chemically crosslinked xylan- $\beta$ -Cyclodextrin hydrogel for the in vitro delivery of curcumin and 5-Fluorouracil. *Int J Biol Macromol* 158:18–31
26. Gupta N, Shivakumar H (2012) Investigation of swelling behavior and mechanical properties of a pH-sensitive superporous hydrogel composite. *Iran J Pharm Sci* 11:481–485
27. Akhlaq M, Ullah I, Nawaz A, Safdar M, Azad A, Abbas S, Helaluddin (2020) Targeted Delivery of Methotrexate through pH-sensitive Hydrogel: To Treat Colon Pathology. doi:<https://doi.org/10.20944/preprints202009.0510.v1>.
28. Abad L, Relve L, Aranilla C, Rosa A (2003) Properties of radiation synthesized PVP-kappa carrageenan hydrogel blends. *Radiat Phys Chem* 68:901–908
29. Bashir S, Teo Y, Ramesh S, Ramesh K (2017) Physico-chemical characterization of pH-sensitive N-Succinyl chitosan-g-poly (acrylamide-co-acrylic acid) hydrogels and in vitro drug release studies. *Polym Degrad Stab* 139:38–54
30. Azam F, Ijaz H, Qureshi J (2020) Functionalized crosslinked interpenetrating polymeric network for pH responsive colonic drug delivery. *Int J Polym Mater* 70:646–655
31. Ijaz H, Tulain U, Qureshi J (2018) Formulation and in vitro evaluation of pH-sensitive cross-linked xanthan gum-grafted acrylic acid copolymer for controlled delivery of perindopril erbumine (PE). *Polym Plast Technol Eng* 57:459–470
32. Ijaz H, Tulain U, Azam F, Qureshi J (2019) Thiolation of arabinoxylan and its application in the fabrication of pH-sensitive thiolated arabinoxylan grafted acrylic acid copolymer. *Drug Dev Ind Pharm* 45(5):754–766

**Publisher's Note** Springer Nature remains neutral with regard to jurisdictional claims in published maps and institutional affiliations.